The International Journal of Advanced Manufacturing Technology (2018) 96:2471–2478
https://doi.org/10.1007/s00170-018-1814-3

ORIGINAL ARTICLE

A generalized dynamic model for spindle vibration influencing surface topography in different ultra-precision machining processes

Zengwen Dong[1] · Shaojian Zhang[1] · Zhiwen Xiong[1] · Xixin Rao[1]

Received: 15 October 2017 / Accepted: 14 February 2018 / Published online: 23 February 2018

Abstract
Ultra-precision machining (UPM) typically involves ultra-precision diamond turning (UPDT), ultra-precision raster milling (UPRM), and ultra-precision grinding (UPG). In UPM, spindle vibration (SV) is a natural feature majorly influencing surface topography. In this paper, a dynamic model for SV was generalized to study its distinctive effects on surface topography in different UPM processes. The theoretical results were identified well by a series of cutting tests. In UPDT, constant cutting forces induce harmonic SV to produce regular patterns. In UPRM, periodical impulsive cutting forces cause periodical impulsive SV to generate quasi-regular patterns. In UPG, random impulsive cutting forces result in partially random impulsive SV to form partially random patterns. The generalized model can be employed to predict the effects of SV on surface generation in UPM.

Keywords Surface topography · Spindle vibration · Ultra-precision machining

Nomenclature

$o(xyz)$	Fixed coordinate system
$O(XYZ)$	Inertial coordinate system
$x/y/z$	Displacement in $O(XYZ)$
$\dot{x}/\dot{y}/\dot{z}$	Velocity in $O(XYZ)$
$\ddot{x}/\ddot{y}/\ddot{z}$	Acceleration in $O(XYZ)$
θ	Rotation angle around x in $o(xyz)$
φ	Rotation angle around y in $o(xyz)$
Ω	Rotation angle around z in $o(xyz)$
$\dot{\theta}$	Angular velocity in $o(xyz)$
$\dot{\varphi}$	Angular velocity in $o(xyz)$
$\dot{\Omega}$	Angular velocity in $o(xyz)$
$\ddot{\theta}$	Angular acceleration in $o(xyz)$
$\ddot{\varphi}$	Angular acceleration in $o(xyz)$
$\ddot{\Omega}$	Angular acceleration in $o(xyz)$
m	Spindle shaft mass
$X/Y/Z$	Machine-tool motion direction in $O(XYZ)$
l_1/l_2	Distance from the equilibrium center to air bearings along the Z-axis
$J_x/J_y/J_z$	Inertial tensor in $o(xyz)$
ω	Spindle speed
f_r	Feed rate
S_r	Step distance
R	Radius of air bearing
r	Tool nose radius
F_x / F_y / F_z	Cutting force in $O(XYZ)$
K	Angular stiffness
B/C	Machine-tool rotational axis
X/Y/Z	Machine-tool slide axis
k_z	Axial stiffness
k_x/k_y	Radial stiffness
d	Depth of cut
d_1	Swing distance
e	Eccentric distance
d_2	Distance from the tool tip to the equilibrium center along the Z-axis
$x_c/y_c/z_c$	Relative distance between tool and workpiece in $O(XYZ)$

1 Introduction

Ultra-precision machining (UPM) was firstly developed to manufacture high quality products in the 1960s [1]. It is one efficient and low-cost means in the most advanced machining technologies. It has widely been employed in manufacturing medical, optical, telecommunication, and photonics products

✉ Shaojian Zhang
S.J.Zhang@connect.polyu.hk

[1] School of Mechatronics Engineering, Nanchang University, Nanchang, Jiangxi, People's Republic of China

[2]. Surface quality can directly reach to sub-micrometric form error and nanometric surface roughness without any subsequent polishing.

Although UPM provides such high surface quality for products, its surface topography is easily affected by a wide variety of factors in a cutting process. The general factors [2] majorly cover cutting conditions [3], tool geometry [3, 4], machine tool [5–7], environmental conditions [8, 9], material factors [10–12], tool wear [13–17], vibration [1, 11, 18–21] etc. In UPM, the vibration is a physical feature as a crucial factor influencing surface topography [1]. It can be categorized into material-induced vibration, tool tip vibration, tool hold vibration, slide vibration, table vibration, and spindle vibration (SV) [1]. Although an ultra-precision machine system has high loop stiffness, its effects on surface topography cannot be ignored, since the SV amplitude can reach up to several decades of nanometers [1].

In UPM, SV yields a crucial impact upon surface topography [19, 20]. Some research has been conducted to study dynamic characteristics of SV and its effects on surface topography in UPM [18–21]. However, dynamic responses of SV in ultra-precision diamond turning (UPDT), ultra-precision raster milling (UPRM), and ultra-precision grinding (UPG) are distinctive due to the different excitation of cutting forces, which are further imprinted at the machined surfaces to produce different surface topographies.

In this study, a dynamic model was generalized to describe SV in different UPM processes, such as UPDT, UPRM, and UPG. The aim was to provide a comprehensive understanding of dynamic responses of SV and its effects on surface topography in different UPM processes. Further, the theoretical results were identified by a series of cutting tests in different UPM processes.

2 Experimental setup

All flat-cutting tests were conducted to study the distinctive effects of SV on surface topographies in different UPM processes, typically including UPDT, UPRM, and UPG. In UPDT (Nanoform 200), the workpiece material was cupro nickel alloy, which was flat-turned with the machining parameters of Table 1. As shown in Fig. 1a, a diamond tool was mounted on a tool fixture with the Z-slide. A workpiece was fixed by a vacuum chuck with an air spindle. The spindle is moved with the X-slide. In the cutting process, the employed diamond tool constantly cuts off surface material. Hence, the cutting forces constantly acted on the spindle.

In UPRM (Precitech Freeform 705G), a copper alloy sample was flat-milled under the machining parameters of Table 2. As shown in Fig. 2b, a diamond tool was clamped with an air spindle moving with the C-axis, the X-slide, and the Y-slide. In addition, a workpiece was setup on the B-axis moving on the Z-slide. In the cutting process, the employed diamond tool periodically intermittently removed off surface material. Hence, the cutting forces periodically intermittently excited the spindle.

Table 1 Machining parameters in UPDT

Spindle speed (ω) (rpm)	2000
Feed rate (f_r) (mm/min)	73
Depth of cut (d) (μm)	25
Tool nose radius (r) (mm)	1.619
Tool rake angle (°)	0
Front clearance angle (°)	15
Workpiece material	Cupro nickel alloy

In UPG (Nanotech 450UPL), the WC workpiece was fixed with a workpiece spindle (C-axis), and flat-grinded with the machining parameters of Table 3. As shown in Fig. 1c, the wheel spindle is fixed on the B-axis and the Z-slide and the workpiece spindle is fixed on the X-slide. In the cutting process, due to the random distribution of the diamond grits on the wheel, surface material was randomly removed off. Hence, the cutting forces randomly intermittently acted on the spindle. All machined flat surfaces were measured by an Optical Profiling System (WYKO NT8000) to detect surface topographies under the effects of SV.

3 Generalized model of spindle vibration

In UPDT, as shown in Fig. 1a, X represents the cutting direction, Y is the feed direction, and Z is the thrust direction (depth of cut direction). F_x is the main cutting force, F_y is the feed cutting force, and F_z is the thrust cutting force. During UPDT, the cutting forces constantly act on the air spindle.

In UPRM, as shown in Fig. 1b, X represents the feed direction, Y is the cutting direction, and Z is the thrust direction (depth of cut direction). F_x is the feed cutting force, F_y is the main cutting force, and F_z is the thrust cutting force. During UPRM, the employed diamond tool intermittently removes workpiece material at the frequency of $1/\omega$ where ω is the spindle speed, so the cutting forces are pulse-like to excite the air spindle.

In UPG, as shown in Fig. 1c, X represents the thrust direction, Y is the cutting direction, and Z is the feed direction (depth of cut direction). F_x is the thrust cutting force, F_y is the main cutting force, and F_z is the feed cutting force. During UPG, the diamond grits randomly distribute on the wheel to contact workpiece, so the cutting forces randomly act on the air spindle.

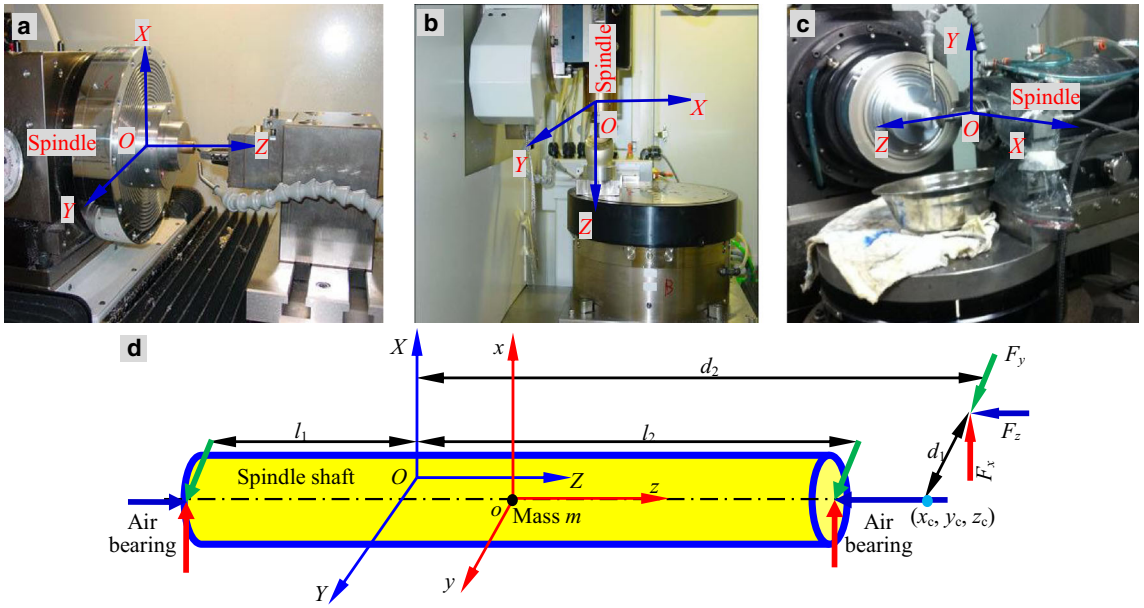

Fig. 1 Spindle vibration in **a** UPDT, **b** UPRM, and **c** UPG with **d** a generalized model

As shown in Fig. 1, the air spindle is modeled as a five-DOF mass-spring-damper system according to Ref. [20]. The axial stiffness of air bearing is denoted by k_z. k_x and k_y are the radial stiffness of air bearing. $K = (k_x + k_y)(l_1^2 + l_2^2) + k_z R^2$ is the angular stiffness of air bearing, where R is the radius of air bearing. m is the mass of spindle shaft. e represents the eccentric distance, which is equal to zero after balancing.

θ, ϕ, and Ω (ωt) are the precession, nutation, and spin angles in the fixed coordinate system $o(xyz)$, respectively. $\dot{\theta}$, $\dot{\phi}$, and $\dot{\Omega}$ (ω) are the corresponding angular velocities, respectively. $\ddot{\theta}$, $\ddot{\phi}$, and $\ddot{\Omega}$ (0) are the corresponding angular accelerations, respectively. x, y, and z are the displacements in the inertial coordinate system $O(XYZ)$, $\dot{x}$, $\dot{y}$, and $\dot{z}$ are the corresponding velocities, and $\ddot{x}$, $\ddot{y}$, and $\ddot{z}$ are the corresponding accelerations, respectively.

J_x, J_y, and J_z are the inertial moments of spindle shaft in $o(xyz)$, respectively. d_1 and d_2 are the distances from the tool tip to the equilibrium center along the Y-axis and the Z-axis, respectively. d_1 is also named the swing distance. l_1 and l_2 are the distances from the equilibrium center to air bearings on two sides along the Z-axis. In UPM, SV can be considered as a transient response to influence surface generation. Hence, damping is not taken into consideration in this study. Based on Newton-Euler equations, a generalized model for SV is expressed as Eq. 1.

$$\begin{bmatrix} \ddot{x} \\ \dot{x} \\ \ddot{y} \\ \dot{y} \\ \ddot{z} \\ z \\ \ddot{\theta} \\ \dot{\theta} \\ \ddot{\phi} \\ \dot{\phi} \end{bmatrix} = \begin{bmatrix} 0 & \frac{-k_x}{m} & 0 & 0 & 0 & 0 & 0 & 0 & 0 & 0 \\ 1 & 0 & 0 & 0 & 0 & 0 & 0 & 0 & 0 & 0 \\ 0 & 0 & 0 & \frac{-k_y}{m} & 0 & 0 & 0 & 0 & 0 & 0 \\ 0 & 0 & 1 & 0 & 0 & 0 & 0 & 0 & 0 & 0 \\ 0 & 0 & 0 & 0 & 0 & \frac{-k_z}{m} & 0 & 0 & 0 & 0 \\ 0 & 0 & 0 & 0 & 1 & 0 & 0 & 0 & 0 & 0 \\ 0 & 0 & 0 & 0 & 0 & 0 & 0 & \frac{-K}{J_x} & \frac{J_y - J_z}{J_x \omega^{-1}} & 0 \\ 0 & 0 & 0 & 0 & 0 & 0 & 1 & 0 & 0 & 0 \\ 0 & 0 & 0 & 0 & 0 & 0 & \frac{J_z - J_x}{J_y \omega^{-1}} & 0 & 0 & \frac{-K}{J_y} \\ 0 & 0 & 0 & 0 & 0 & 0 & 0 & 0 & 1 & 0 \end{bmatrix} \begin{bmatrix} \dot{x} \\ x \\ \dot{y} \\ y \\ \dot{z} \\ z \\ \dot{\theta} \\ \theta \\ \dot{\phi} \\ \phi \end{bmatrix} + \begin{bmatrix} 1 & 0 & 0 \\ 0 & 0 & 0 \\ 0 & 1 & 0 \\ 0 & 0 & 0 \\ 0 & 0 & 1 \\ 0 & 0 & 0 \\ \frac{d_2 \sin\Omega}{-J_x} & \frac{d_2 \cos\Omega}{J_x} & \frac{d_1 \cos\Omega}{J_x} \\ 0 & 0 & 0 \\ \frac{d_2 \cos\Omega}{J_y} & \frac{d_2 \sin\Omega}{J_y} & \frac{d_1 \sin\Omega}{J_y} \\ 0 & 0 & 0 \end{bmatrix} \begin{bmatrix} F_x \\ F_y \\ F_z \end{bmatrix} \quad (1)$$

Table 2 Machining parameters in UPRM

Spindle speed (ω) (rpm)	4000
Feed rate (f_r) (mm/min)	80
Depth of cut (d) (μm)	5
Swing distance (d_1) (mm)	28.48
Step distance (S_r) (μm)	10
Tool nose radius (r) (mm)	0.619
Tool rake angle (°)	0
Front clearance angle (°)	15
Cutting strategy	Horizontal cutting
Cutting mode	Up-cutting
Workpiece material	Copper alloy

In Eq. 1, the dynamic responses of SV (x, y, z, θ, and ϕ) change the relative distance (x_c, y_c, z_c) between tool and workpiece, which is reproduced at the machined surface further to affect surface topography. In this study, x, y, z, θ, and ϕ are regarded as linear small quantities, so their quadratic small quantities are considered equal to zero. Therefore, the relative distance (x_c, y_c, z_c) between tool and workpiece is simplified and expressed as follows:

$$\begin{bmatrix} x_c \\ y_c \\ z_c \end{bmatrix} = \begin{bmatrix} x + \phi d_2 \\ y + \theta d_2 \\ z \end{bmatrix} \tag{2}$$

4 Results and discussion

Eq. 1 is a generalized dynamic model to express SV under the excitation of cutting forces in UPDT, UPRM, and UPG. It is

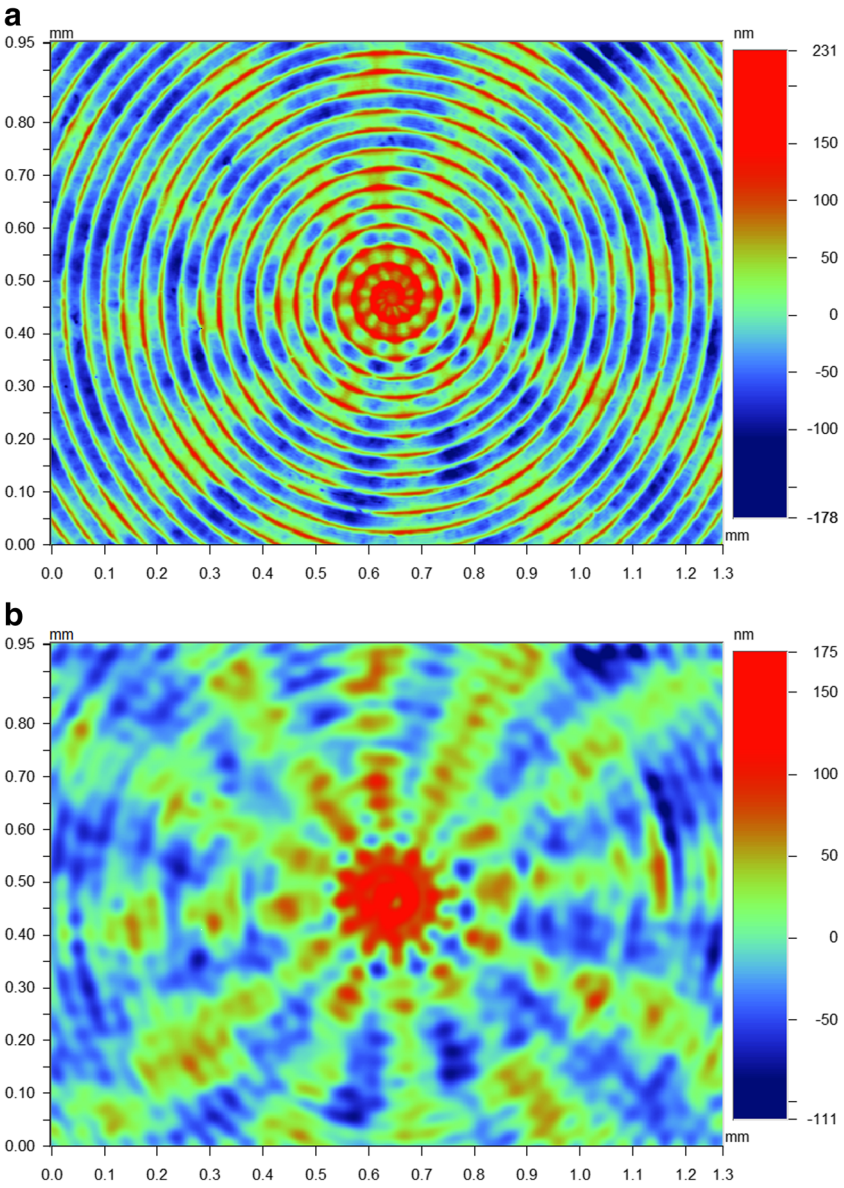

Fig. 2 Machined surface in UPDT. **a** Surface topography. **b** Filtered surface topography with Fourier filter window of rectangle at low pass of 25 mm^{-1}

Table 3 Machining parameters in UPG

Wheel spindle speed (ω) (rpm)	20,000
Feed rate (f_r) (mm/min)	0.5
Workpiece spindle speed (rpm)	120
Depth of grinding (d) (μm)	0.5
Wheel size (diameter) (mm)	20
Diamond grit (#)	1500
Distribution (%)	75
Workpiece material	WC carbide

made up of three parts, input (cutting forces), state space (the SV system), and output (dynamic responses). From Eq. 1, the state space is the natural feature of SV, which involves axial SV, radial SV, and coupled-tilting SV with the corresponding frequencies. The dynamic responses (output) of SV are influenced by the external excitation of cutting forces (input). The relative distance (x_c, y_c, z_c) between tool and workpiece expressed in Eq. 2 is determined by the dynamic responses (x, y, z, θ, and ϕ) in Eq. 1. It is reproduced at the machined surface further to affect surface topography. Therefore, in UPDT, UPRM, and UPG, the cutting forces are different to yield distinctive surface patterns at the machined surfaces.

In UPDT, the cutting forces are considered constant to act on the spindle, so the SV is harmonic. The dynamic responses are harmonic to result in the harmonic relative distance, which is imprinted at the machined surface. Therefore, the SV produces regular patterns at the machined surface. In UPRM, the cutting forces intermittently and periodically excite the spindle to cause periodical impulsive SV. The dynamic responses are periodically impulsive, which further result in the periodically impulsive

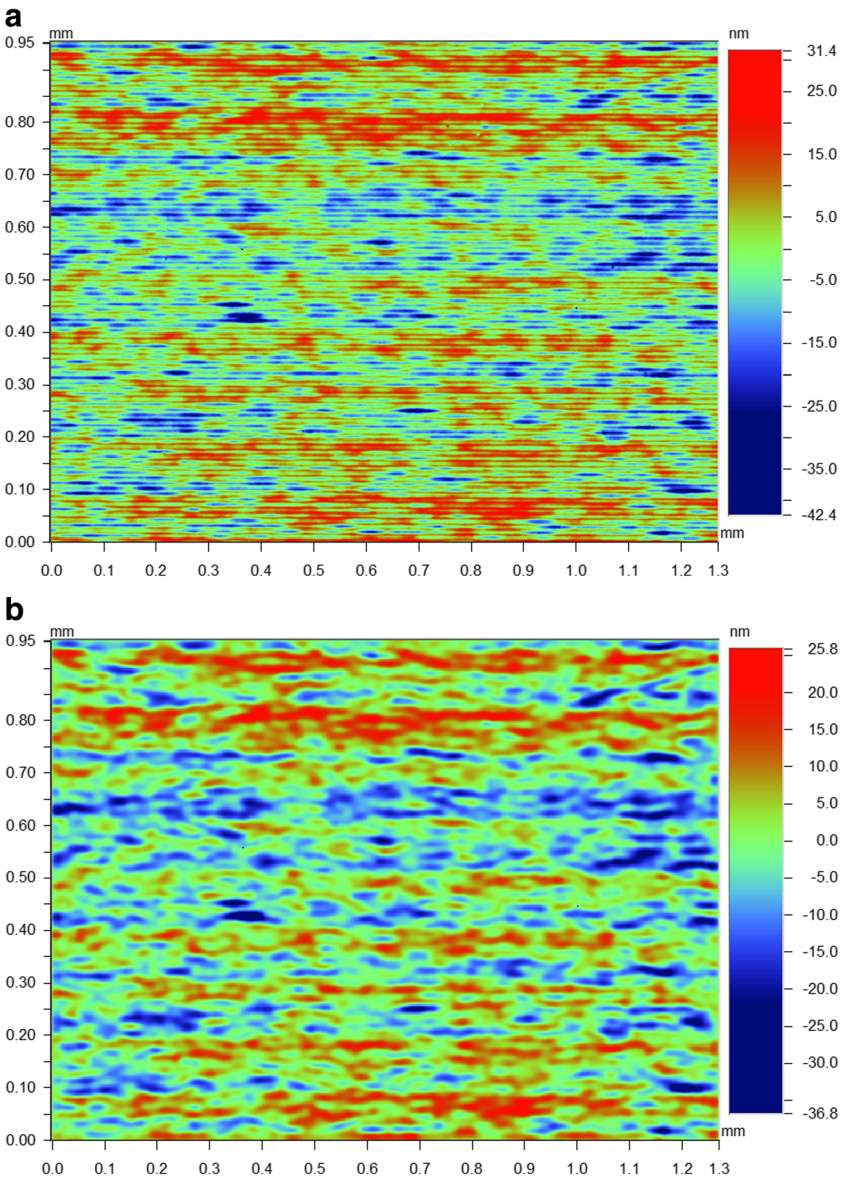

Fig. 3 Machined surface in UPRM. **a** Surface topography. **b** Filtered surface topography with Fourier filter window of rectangle at low pass of 48 mm^{-1}

relative distance. Consequently, the SV produces quasi-regular patterns at the machined surface. In UPG, the cutting forces randomly excite the spindle to induce partially random impulsive SV since the diamond grits randomly distribute at the grinding wheel. The dynamic responses are partially random, which further induce the partially random relative distance. Resultantly, the surface patterns are partially random at the machined surface.

To identify the distinctive patterns produced by the distinctive SV, a series of flat-cutting tests were carried out in UPDT, UPRM, and UPG, respectively. The machining parameters are listed in Tables 1, 2, and 3, respectively. The flat-cut surfaces were measured by Wyko NT8000. The measured surface topographies were filtered with Fourier filter window of rectangle at low pass provided by the measurement system software to reduce other's effects, such as material factors and tool marks, whose high spatial frequency is determined by machining parameters in UPDT, UPRM, and UPG. Therefore, different low passes were adopted for the machined surfaces of UPDT, UPRM, and UPG and it was easy to detect the effects of SV on surface topographies by filtering the high spatial frequency effects. The results are shown in Figs. 2, 3, and 4. Figure 2a shows the flat surface machined after UPDT. The radial patterns and spiral tool marks are clear. Figure 2b clearly presents the radial patterns are periodical. Hence, it indicates that in UPDT, the SV is harmonic to produce periodical radial patterns at the turned surface.

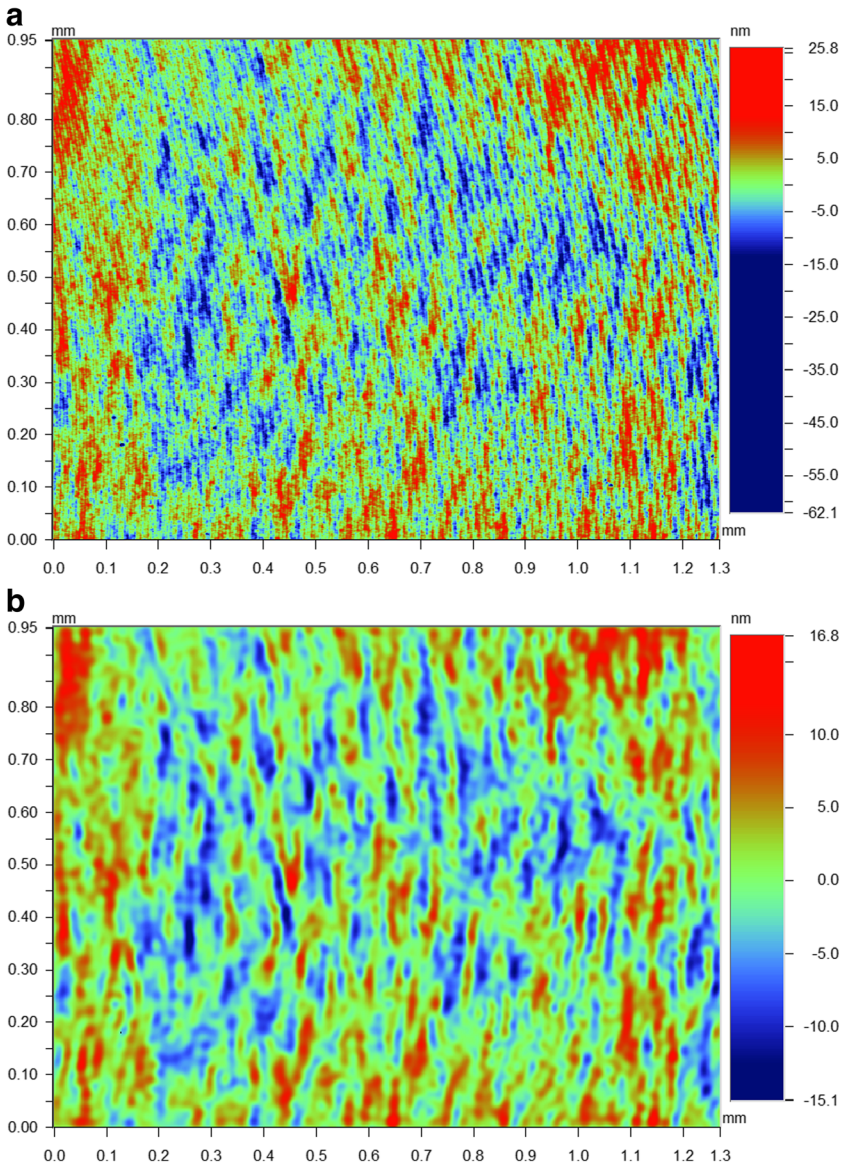

Fig. 4 Machined surface in UPG. **a** Surface topography. **b** Filtered surface topography with Fourier filter window of rectangle at low pass of 40 mm^{-1}

Figure 3a demonstrates the milled flat surface after UPRM. The milled flat surface shows stripe patterns and tool marks. In Fig. 3b, the ribbon stripes are quasi-regular. The kind of quasi-regular patterns were formed at the milled surface in UPRM. Therefore, it means that in UPRM, the SV is periodically impulsive to produce quasi-regular patterns at the milled surface. Figure 4a depicts the grinded flat surface after UPG. It shows the irregular/random patterns and tool marks. In Fig. 4b, the partially random patterns are clearly presented. Hence, it reveals that in UPG, the SV is randomly impulsive to produce partially random patterns at the grinded surface.

Overall, in UPDT, the SV is harmonic due to the constant excitation of cutting forces, which produces regular patterns at the machined surface. In UPRM, the SV is periodically impulsive due to the periodical intermittent excitation of cutting forces, which forms quasi-regular patterns at the machined surface. In addition, in UPG, the SV is random due to the random excitation of cutting forces, which generates partially random patterns at the machined surface. All are well supported by Eq. 1 and Eq. 2.

5 Conclusions

Spindle vibration (SV) has a key impact upon surface topography at the machined surface. In this study, a generalized dynamic model was developed to study SV and its effects on surface generation in different UPM processes, involving ultra-precision diamond turning (UPDT), ultra-precision raster milling (UPRM), and ultra-precision grinding (UPG). The first study looking at the distinctive effects of SV in different UPM processes on surface topography has been completed, which provides an in-depth understanding so that the key results can be achieved as follows:

(i) A dynamic model is generalized well to represent SV in different UPM processes. The SV system is linear and harmonic, which includes axial SV, radial SV, and coupled-tilting SV. Its dynamic responses are determined by the external excitation of cutting forces in UPM.

(ii) In UPDT, regular patterns are generated since constant cutting forces induce harmonic SV. In UPRM, quasi-regular patterns are produced since periodical impulsive cutting forces cause impulsive SV. In UPG, partially random patterns are formed since random impulsive cutting forces partially random impulsive SV.

(iii) Further, the generalized dynamic model can be employed to predict the effects of SV on surface topography/generation and further to analyze surface roughness and form error. Significantly, it is a potential theoretical method to improve surface quality in UPM.

Funding information This work was supported by the National Natural Science Foundation of China (Grants no. 51405217), the Science Foundation of Jiangxi Province of China (Grants no. 20161BBE50055 and 20142BAB216025), and the Youth Science Foundation of Jiangxi Educational Committee of China (Grant no. GJJ4210).

References

1. Zhang SJ, To S, Zhang GQ, Zhu ZW (2015) A review of machine-tool vibration and its influence upon surface generation in ultra-precision machining. Int J Mach Tools Manuf 91:34–42
2. Zhang SJ, To S, Wang SJ, Zhu ZW (2015) A review of surface roughness generation in ultra-precision machining. Int J Mach Tools Manuf 91:76–95
3. Cheung CF, Lee WB (2000) Study of factors affecting the surface quality in ultra-precision diamond turning. Mater Manuf Process 15(4):481–502
4. Chen X, Xu J, Fang H, Tian R (2017) Influence of cutting parameters on the ductile-brittle transition of single-crystal calcium fluoride during ultra-precision cutting. Int J Adv Manuf Technol 89(1–4):219–225
5. Takeuchi Y, Sakaida Y, Sawada K, Sata T (2000) Development of a 5-axis control ultraprecision milling machine for micromachining based on non-friction servomechanisms. CIRP Ann Manuf Technol 49:295–298
6. Chen W, Lu L, Yang K, Huo D, Su H, Zhang Q (2015) A novel machine tool design approach based on surface generation simulation and its implementation on a fly cutting machine tool. Int J Adv Manuf Technol 80:829–837
7. Chen W, Luo X, Su H, Wardle F (2016) An integrated system for ultra-precision machine tool design in conceptual and fundamental design stage. Int J Adv Manuf Technol 84(5–8):1177–1183
8. Wang SJ, To S, Chan CY, Cheung CF, Lee WB (2010) A study of the cutting-induced heating effect on the machined surface in ultra-precision raster milling of 6061 Al alloy. Int J Adv Manuf Technol 51:69–78
9. Wang SJ, To S, Chen X, Chen XD (2015) An investigation on surface finishing in ultra-precision raster milling of aluminum alloy 6061. Proc Inst Mech Eng Part B-J Eng Manuf 229(8):1289–1301
10. Fang FZ, Liu YC (2004) On minimum exit-burr in microcutting. J Micromech Microeng 14:984–988
11. Sun Y, Chen W, Liang Y, An C, Chen G, Su H (2015) Dynamic error budget analysis of an ultraprecision fly cutting machine tool. Int J Adv Manuf Technol 76:1215–1224
12. Peng Y, Jiang T, Ehmann KF (2014) Research on single-point diamond fly-grooving of brittle materials. Int J Adv Manuf Technol 75:1577–1586
13. Chen Y-L, Cai Y, Shimizu Y, Ito S, Gao W, Ju B-F (2016) On-machine measurement of microtool wear and cutting edge chipping by using a diamond edge artifact. Precis Eng 43:462–467
14. Evans CJ, Browy EC, Childs THC, Paul E (2015) Interferometric measurements of single crystal diamond tool wear. CIRP Ann Manuf Technol 64:125–128
15. Chen Y-L, Wang S, Shimizu Y, Ito S, Gao W, Ju B-F (2016) An in-process measurement method for repair of defective microstructures by using a fast tool servo with a force sensor. Precis Eng 39:134–142

16. Zhou X, Zuo C, Liu Q, Lin J (2016) Surface generation of freeform surfaces in diamond turning by applying double-frequency elliptical vibration cutting. Int J Mach Tools Manuf 104:45–57
17. Chan CY, Li LH, Lee WB, Wong HC (2016) Monitoring life of diamond tool in ultra-precision machining. Int J Adv Manuf Technol 82(5–8):1141–1152
18. An CH, Zhang Y, Xu Q, Zhang FH, Zhang JF, Zhang LJ, Wang JH (2010) Modeling of dynamic characteristic of the aerostatic bearing spindle in an ultra-precision fly cutting machine. Int J Mach Tools Manuf 50:374–385
19. Zhang SJ, To S, Cheung CF, Wang HT (2012) Dynamic characteristics of an aerostatic bearing spindle and its influence on surface topography in ultra-precision diamond turning. Int J Mach Tools Manuf 62:1–12
20. Zhang SJ, To S, Wang HT (2013) A theoretical and experimental investigation into five-DOF dynamic characteristics of an aerostatic bearing spindle in ultra-precision diamond turning. Int J Mach Tools Manuf 71:1–10
21. Chen D, Gao X, Dong L, Fan J (2017) An evaluation system for surface waviness generated by the dynamic behavior of a hydrostatic spindle in ultra-precision machining. Int J Adv Manuf Technol 91(5–8):2185–2192